

**ENEL 698**

GRADUATE PROJECT

PROJECT REPORT ON

**DESIGN AND IMPLEMENTATION OF A  
SOLID STATE STREET LIGHTING SYSTEM**

Prepared By:

**Arjuna Kodisinghe**  
(255373)

Supervisor:

**Dr. Dave Irvine-Halliday**

April, 2008

## **Abstract**

Many areas in the developing countries are without electricity [1]. As a result, street/outdoor lighting is severely limited and it is identified that provisioning of conventional electric street lighting in those areas in the near future would be a difficult prospect. As discussed in [4] & [5], street/pathway lighting is an important public service that provides a safer environment to its users. Therefore, lack of street lighting may translate into a lower quality of life. Apart from the regular populated areas, these living conditions are gravely compromised in such places like refugee camps [19] where properly lit outdoors could make a significant difference.

Having identified this problem, a self-sustained electric street lighting system using solid state lighting devices is proposed as a potential resolution. This lighting system is designed to be scalable to meet varied lighting requirements. In this report, the proposed lighting system is discussed in detail and the results are presented.

## **Acknowledgments**

I would like to take this opportunity to thank my supervisor, Dr. Dave Irvine-Halliday for his continuous guidance throughout this exercise and always reminding me to think like a practical engineer.

My sincere gratitude also goes to Ganesh Doluweera at University of Calgary for providing me with great technical support and direction.

I would also like to express my heartfelt thanks to my friends at work: Niel Rao and Carl Duddin for helping me build the lamp post.

Last, but never the least, I am indebted to my lovely wife Arosha for allowing me to work on this project long hours while encouraging me right throughout and my dearest kids Venuja & Disara for not complaining when I couldn't find time to play with you.

# Table of Contents

<b>Abstract.....</b>	<b>ii</b>
<b>Acknowledgments .....</b>	<b>iii</b>
<b>Table of Contents .....</b>	<b>iv</b>
<b>List of Figures.....</b>	<b>vii</b>
<b>List of Tables .....</b>	<b>viii</b>
<b>Chapter One - Introduction to Street Lighting.....</b>	<b>1</b>
1.1 History of Electric Street Lighting .....	1
1.2 Importance of Street Lighting .....	1
1.3 North American Street Lighting Standards.....	2
<b>Chapter Two - Project Scope .....</b>	<b>4</b>
2.1 Objectives .....	4
2.2 Solid-State Street Lighting Advantage .....	4
2.3 Potential Concerns with Solid-State Street Lighting Systems .....	5
<b>Chapter Three - System Parameter Estimation.....</b>	<b>7</b>
<b>Chapter Four - System Design Details .....</b>	<b>11</b>
4.1 PV Panel.....	11
4.2 SLA Battery .....	11
4.3 LED Driver .....	12

4.3.1 Soft start .....	18
4.3.2 Handling WLED failures .....	19
4.3.3 Driver Efficiency .....	20
4.4 Controller .....	21
4.4.1 Quiescent Power Consumption.....	22
4.4.2 Minimizing false triggers.....	23
4.4.3 Software Design.....	24
4.5 Battery Charger Module .....	24
4.5.1 Charging Algorithm.....	25
4.5.2 Bulk Charge Mode.....	25
4.5.3 Overcharge Mode.....	27
4.5.4 Float Charge Mode .....	28
4.5.5 Battery Charger Efficiency .....	28
4.5.6 Battery Protection .....	29
4.6 White Light Emitting Diodes (WLED).....	29
4.6.1 Thermal Calculations .....	30
4.7 Optical Modifiers .....	31
4.8 Luminaire/Lamp Post.....	32
<b>Chapter Five - System Scalability and Adaptability .....</b>	<b>33</b>
5.1 Total Lumen Output.....	33

5.2 Illumination distribution .....	33
<b>Chapter Six - Cost Analysis .....</b>	<b>35</b>
6.1 LCC and ALCC for One WLED branch.....	36
6.2 LCC and ALCC for Two WLED Branches .....	37
<b>Chapter Seven - Field Measurements .....</b>	<b>38</b>
<b>Chapter Eight - Conclusion and Future work .....</b>	<b>41</b>
<b>Appendix A - Component list and pricing.....</b>	<b>43</b>
<b>Appendix B - C language source code for PIC12F675 microcontroller .....</b>	<b>47</b>
<b>Appendix C – Field Illuminance Measurement Data .....</b>	<b>50</b>
<b>References.....</b>	<b>51</b>

## List of Figures

Figure 1: Lighting fixture types .....	2
Figure 2: Depth of Discharge versus battery life .....	12
Figure 3: LDO current regulator .....	13
Figure 4: Components of a buck regulator .....	14
Figure 5: WLED Driver and Controller Schematic .....	16
Figure 6: Amplification of current-sense voltage .....	17
Figure 7: WLED Driver MOSFET gate waveforms .....	19
Figure 8: WLED Driver inputs and outputs.....	20
Figure 9: Battery Charger Schematic.....	26
Figure 10: Bulk charge mode – MOSFET gate waveforms .....	27
Figure 11: Over charge mode – MOSFET gate waveforms .....	28
Figure 12: Float charge mode – MOSFET gate waveform.....	28
Figure 13: Light Distribution Characteristics of Flare Lens by L2Optics .....	31
Figure 14: Spatial Illumination Distribution and Lens Orientation .....	34
Figure 15: Digital photos of the street lamp during the field measurements .....	38
Figure 16: Vertical Illuminance distribution (Lux) vs. the distance along the street .....	39
Figure 17: Vertical Illuminance distribution (Lux) vs. the distance across the street .....	40

## List of Tables

Table 1: IESNA Recommended values for Low Pedestrian Conflict Areas .....	3
Table 2: IESNA Recommended values for Medium Pedestrian Conflict Areas .....	3
Table 3: IESNA Recommended values for High Pedestrian Conflict Areas.....	3
Table 4: Parameter Summary for two possible configurations.....	10
Table 5: WLED Driver Efficiency Measurements .....	21
Table 6: Battery Charger Efficiencies.....	29
Table 7: Capital Cost Breakdown.....	35
Table 8: Capital Cost Breakdown for 6 WLEDs .....	35
Table C1 – Measured Vertical Illuminance Distribution along the Street.....	50
Table C2 – Measured Vertical Illuminance Distribution across the Street .....	50

# **Chapter One - Introduction to Street Lighting**

Street lighting can be defined as the artificial illumination of streets and pathways when available natural light (sunlight) drops below a pre-determined level. Street lighting dates back to pre-electricity era. A brief history on first electric street lighting is given below.

## **1.1 History of Electric Street Lighting**

The very first electric street lamp was based on electric arc lamps [2]. The first instance of permanent public street lighting (electrical) anywhere in the world was in the Public Square of Cleveland, a little park of about 10 acres. In April 1879, twelve arc lamps at 2000 candlepower were installed in the park. Since the arc lamps were very bright sources, they had to be mounted on very high poles. Some of these poles were higher than 200 feet. Since the carbon electrode burns away at a fast rate in the arc lamp they were maintenance-intensive. These arc lamps were soon replaced by cheap, longer lasting and bright incandescent lamps. Most of the today's street lamps use high intensity discharge lamps such as HPS (high pressure sodium lamps) [3].

## **1.2 Importance of Street Lighting**

Street lighting is an essential public service that provides a safer environment to its users.

Proper use of roadway lighting as an operative tool provides economic and social benefits to the public including [4]:

- (a) Reduction in night accidents, attendant human misery and economic loss
- (b) Aid to police protection and enhanced sense of personal security
- (c) Facilitation of traffic flow
- (d) Promotion of business and the use of public facilities during the night hours.

While this service is commonly available in developed countries, there is a shortage of proper street lighting facilities in many areas in developing countries due to lack of financial resources. The lack of adequate light at night has given rise to poor living conditions and as such, wildlife encounters, street crimes, and other mishaps are commonplace [5].

### 1.3 North American Street Lighting Standards

Illumination Engineering Society of North America (IESNA) has published roadway lighting specifications in IESNA RP-8-00 American National Standard Practice for Roadway Lighting (reaffirmed 2005). Roadways are categorized from local walkways to expressways and different illumination levels and illumination patterns have been recommended. Fixtures for roadway application are classified as type I, II, III or IV (Figure 1). Type I fixtures are generally used for narrow roadways. Type IV is used for wide, multi-lane roads.

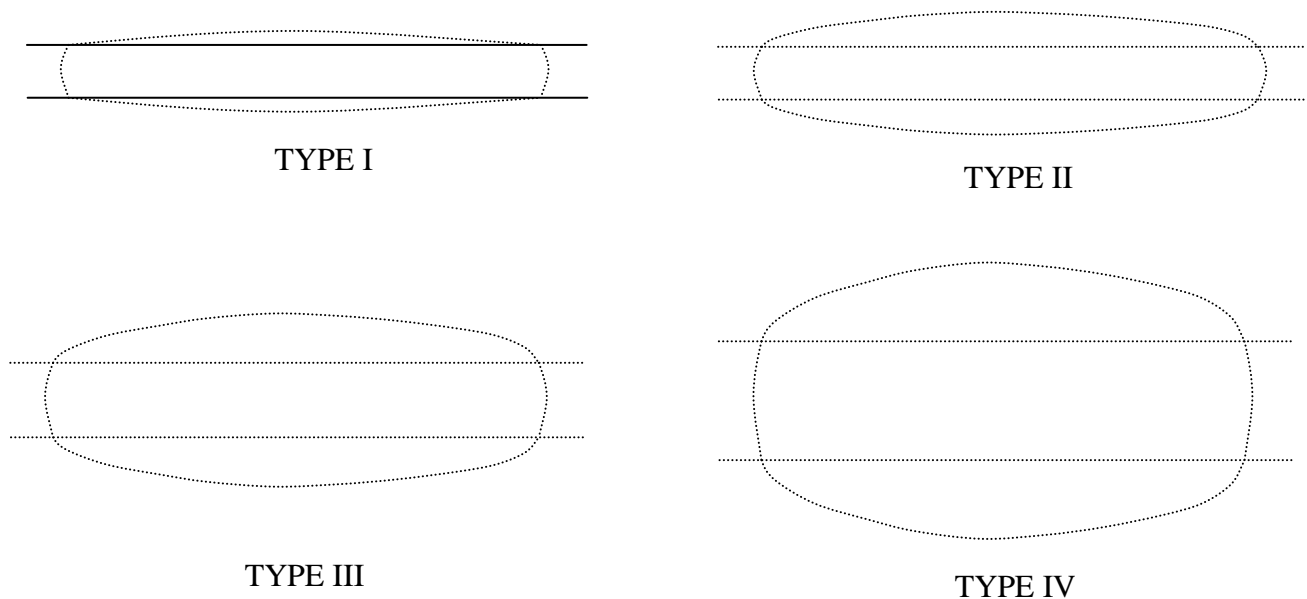


**Figure 1: Lighting fixture types (SOURCE: IESNA Lighting Handbook [4])**

Tables 1 through 3 show some of the IESNA recommended illuminance values.

**Maintained Illuminance Values for Walkways/Bikeways**

	$E_H$ (Lux)	$E_{Vmin}$ (Lux)	$E_{avg}/E_{min}^*$
<b>Rural/Semi-Rural Areas</b>	2.0	<b>0.6</b>	10.0
<b>Low Density Residential</b>	3.0	0.8	6.0
<b>Medium Density Residential</b>	4.0	1.0	4.0

**Table 1: IESNA Recommended values for Low Pedestrian Conflict Areas**

**Maintained Illuminance Values for Walkways/Bikeways**

	$E_H$ (Lux)	$E_{Vmin}$ (Lux)	$E_{avg}/E_{min}^*$
<b>Pedestrian Areas</b>	5.0	2.0	4.0

**Table 2: IESNA Recommended values for Medium Pedestrian Conflict Areas**

**Maintained Illuminance Values for Walkways/Bikeways**

	$E_H$ (Lux)	$E_{Vmin}$ (Lux)	$E_{avg}/E_{min}^*$
<b>Mixed Vehicle &amp; Pedestrian**</b>	20.0	10.0	4.0
<b>Pedestrian Only</b>	10.0	5.0	4.0

**Table 3: IESNA Recommended values for High Pedestrian Conflict Areas**

Notes:

\* Horizontal Only

\*\* Mixed vehicle and pedestrian refers to those areas where the pedestrians are immediately adjacent to vehicular traffic without barriers or separation.

$E_H$ =Average horizontal illuminance at walkway/bikeway

$E_{Vmin}$ =Minimum vertical illuminance at 1.5m above walkway/bikeway measured in both directions parallel to the main pedestrian flow.

## **Chapter Two - Project Scope**

### **2.1 Objectives**

The goal of this project is to introduce a practical solution to outdoor/street lighting to developing countries and/or financially challenged and/or resource-limited areas of the world. Meeting the international standards for illumination levels is not the primary objective, rather, providing the users with a ‘useful’ and economical lighting system is. Also, types of the roadways under consideration are limited to narrow walkways/bikeways and two-lane motorways without a centre median island. More priority is given to pedestrians’ requirements than motorists as it is assumed vehicular traffic on these roads is minimal.

The proposed lighting system is to be operated without relying on an existing electrical power source (e.g. national grid). A renewable power source, solar power, is used to power this system. The reason for using solar power is because it is typically more predictable than other renewable energy sources such as wind energy. Further, the ability to harness solar energy using solid-state photo voltaic (PV) panels brings in other advantages discussed below.

### **2.2 Solid-State Street Lighting Advantage**

As the name suggests, all the main components of the proposed system consist of solid-state devices. The inherent advantage of solid-state devices is that they have a longer life span and less regular maintenance work over the life span due to lack of mechanical or moving elements.

Apart from the solid-state electronic components, the main solid-state items in the system are the solar photo voltaic panel, the rechargeable battery and the light emitting diodes (LED). Solar PV panels typically have a minimum useful life expectancy of 20 years [7] and today’s WLEDs feature lumen maintenance of 70% after 50 000 hours of use [8]. This lighting solution does not

rely or make use of external power source such as the national grid. Instead, it contains its own power generation and storage modules. Thus, this system can be deployed in almost any remote location. Also, since this system depends on minimum infrastructure needs it can be deployed rapidly in a matter of days. This makes this system ideal for places like refugee camps [20] where ad-hoc installations are necessary.

In conventional outdoor lighting systems where sodium vapor lamps are used, the output light has very poor color reproduction (near zero CRI). This issue is easily circumvented by using white LEDs that produce light very close to natural white light. The high CRI value (around 82) of WLEDs allows the users to easily distinguish objects by their color. Another advantage of using LEDs over conventional lighting sources is that LEDs are inherently rugged by design and can withstand a very high level of abuse. The LEDs light output is directional and therefore the output light distribution is easier to manipulate with external optics so that light can be directed to where it is needed. The WLEDs do not contain hazardous materials such as Mercury and Lead. Therefore, they do not pose health threats when disposed of.

Due to the use of renewable energy source, this environmentally friendly system has zero greenhouse gas emissions to the atmosphere during its operational life (with the exception of the potential greenhouse gas emission during manufacturing and installation of replaceable components such as the rechargeable battery).

### **2.3 Potential Concerns with Solid-State Street Lighting Systems**

WLED is still an emerging technology. Currently, the efficacy of WLEDs is not on par with their conventional counterparts (e.g. for low pressure sodium lamps and WLEDs, the efficacies are approximately 180lm/W and 130lm/W respectively). Therefore, there will be an efficiency penalty in the proposed system. The proposed system has a higher component-count than a

typical lighting installation and as a result, it comes at a higher initial cost and increased system complexity. Another potential issue might arise as a result of a benefit discussed above - the high CRI value of WLEDs. This might hinder a clear observation of the sky at night. This type of 'light pollution' is minimal with typical sodium vapor lamps as their very narrow spectral lines can be easily filtered out in the observing equipment. However, it should be noted that this will become a concern only in the areas where astronomical observatories are located and large scale WLED outdoor lighting systems are deployed. Furthermore, the beam pattern from the LEDs can be manipulated with optical modifiers so that the unnecessary beams can be cut-off to minimize the light pollution.

## Chapter Three - System Parameter Estimation

One of the main goals at the beginning was to scale the system in terms of power and luminous flux requirements. Even though this system is not meant to meet international standards as far as light output is concerned it still had to generate a ‘useful’ amount of light. At the same time, the proposed system should not be extravagantly expensive to make. According to the IESNA guidelines for rural/semi rural areas, the minimum maintained vertical illuminance is 0.6 lux (table 1). However, it was observed that even at 0.1 Lux, the visibility is not totally lost. In fact, the full moon’s illumination is around 0.1~0.2 Lux and it is marginally sufficient to identify people at close proximity. Based on this argument, it was decided to target a minimum (vertical) illuminance of 0.1 Lux at the edge of the street lamp’s beam. In addition, information obtained from an unpublished project done in Nepal (by Muni Raj Upadhyaya et al.) was used when determining the system parameters.

For this implementation, the following requirements/conditions have been assumed:

PV Power =	30	W
Peak Sun Hours =	5.5	Hrs
# of WLEDs =	6	
WLED Efficiency =	85	lm @350mA, @T <sub>j</sub> =85C
Ambient Temperature =	35	C
Wire (18 AWG) resistance =	0.02094	W/m
Maximum height of the light post=	15	feet
Minimum vertical illuminance=	0.1	Lux

The following calculations are used to determine the rest of the system parameters. All potential losses are included to simulate a real-world system. Some important parameters are presented in boldface letters.

**At the Solar PV Panel:**

$$\text{PV Temperature} = (\text{Ambient Temperature} + 15^\circ\text{C}) = 50 \text{ }^\circ\text{C}$$

For every 1C degree increase in the temperature of the PV panel above 25°C,

$$\text{the efficiency is reduced by 0.5\%, } \eta_{\text{PV}} = 88\%$$

$$\text{Actual Power Output} = 26.25 \text{ W}$$

**Wire Losses (Solar PV Panel to Battery Charger):**

$$\text{Wire Length} = 5 \text{ m}$$

$$\text{Max. Current} = 1.7 \text{ A}$$

$$\text{Wire Loss} = 0.30 \text{ W}$$

**At the Battery Charger:**

$$\text{Input Power} = \text{PV Power Output} - \text{Wire Loss} = 25.9474 \text{ W}$$

$$\eta_{\text{CHG}} = 82\%$$

$$\text{Actual Power Output} = 21.2768 \text{ W}$$

**Wire Losses (Battery Charger to Battery):**

$$\text{Wire Length} = 0.5 \text{ m}$$

$$\text{Max. Current} = 1.7 \text{ A}$$

$$\text{Wire Loss} = 0.03 \text{ W}$$

**At the Battery:**

$$\text{Input Energy} = (\text{Battery Charger Power Output} - \text{Wire Losses}) \times \text{Peak Sun}$$

$$\text{Hours} = 116.86 \text{ Wh}$$

$$\eta_{\text{BAT}} = 85\%$$

$$\text{Charging Energy Input} = 99.33 \text{ Wh}$$

$$\text{Discharging Energy Output} = \text{Charging Energy Input} \times \eta_{\text{BAT}} = 84.43 \text{ Wh}$$

Discharging Energy Output should represent 25% DOD per day.

Therefore, the full battery capacity = 4 x Discharging Energy Output / Median

$$\text{voltage} = \text{Battery Capacity based on 25\% DOD} = 26.6 \text{ Ah}$$

$$\text{Discharging Rate} < C/10$$

$$\text{Current Drawn from Battery} = 0.665 \text{ A}$$

**Wire Losses (Battery to LED Driver):**

$$\text{Wire Length} = 0.5 \text{ m}$$

$$\text{Max. Current} = 1 \text{ A}$$

$$\text{Wire Loss} = 0.0105 \text{ W}$$

**At the LED Driver:**

$$\text{Power Demand} = 6.93 \text{ W}$$

$$\eta_{\text{DRV}} = 82\%$$

$$\text{Required Power Input} = 8.45 \text{ W}$$

**Wire Losses (LED Driver to LED Lamps):**

$$\text{Wire Length} = 5 \text{ m}$$

$$\text{Max. Current} = 1 \text{ A}$$

$$\text{Wire Loss} = 0.105 \text{ W}$$

**At the Luminaire:**

$$\text{Input Energy} = 68.80 \text{ Wh}$$

$$\eta_{\text{OPT}} = 90\%$$

$$\text{Typical WLED } V_{\text{FORWARD}} = 3.3 \text{ V}$$

WLED Driving Current =	0.35 A
Typical Power per WLED =	1.155 W
Total Power Consumption =	6.93 W
<b>Streetlight Hrs =</b>	<b>9:55 hh:mm</b>
<b>Max. Light Output =</b>	<b>459 Lumens</b>

In the above exercise almost all the important loss factors have been accounted for to get realistic performance data. The results indicate that approximately 10 hours of street lighting is possible with a 30W solar PV panel and 6 WLEDs. Although this calculation is performed for 6 WLEDs, the output of the system can scale down by a factor of 2 without design modifications while maintaining the same service up time (approximately 10 hrs).

Table 4 summarizes the main system parameters for the two configurations

Parameter	3 WLEDs	6 WLEDs
<b>PV panel</b>	15W	30W
<b>Rechargeable Battery</b>	13Ah	27Ah
<b>Typical Lumen Output</b>	230	460
<b>Service Hours (approx.)</b>	10 Hours	10 Hours
<b>Capital Cost (approx.)</b>	\$250	\$400

**Table 4: Parameter Summary for two possible configurations**

## **Chapter Four - System Design Details**

The proposed system consists of the following components:

1. Photo-Voltaic (PV) panel
2. Sealed Lead-Acid rechargeable battery
3. LED driver
4. Lighting controller
5. Battery charger
6. White Light Emitting Diodes (WLED)
7. Optical modifiers (lenses)
8. Luminaire/Lamp post

### **4.1 PV Panel**

The PV panel acts as the solid-state power generation source for the system. The renewable energy captured during the daylight hours in the PV is transferred into the rechargeable battery via the battery charger for the lighting source to consume at nighttime. This clean, noise-, maintenance- and emission-free solid-state power source has an operational lifespan of about 20 years [7].

### **4.2 SLA Battery**

A Sealed Lead Acid (SLA) battery is chosen because it is more economical compared to other rechargeable battery technologies. The capacity of the SLA battery is discussed in the power budget. A drawback of using SLA batteries is that they cannot be fully discharged between the charge/discharge cycles without adversely affecting their useful life. Therefore, a battery with a much higher capacity (than what is required per cycle) is needed for maintaining a longer battery

life. A good compromise is to discharge the battery down to about 25%. As seen in figure 2, by reducing the depth of discharge (DOD) from 50% to 30%, the battery life is nearly tripled. Low voltage cut-off circuitry is implemented to protect the battery from being over discharged. In addition to the DOD value, the discharge current from a sealed lead acid battery should not be arbitrarily high.

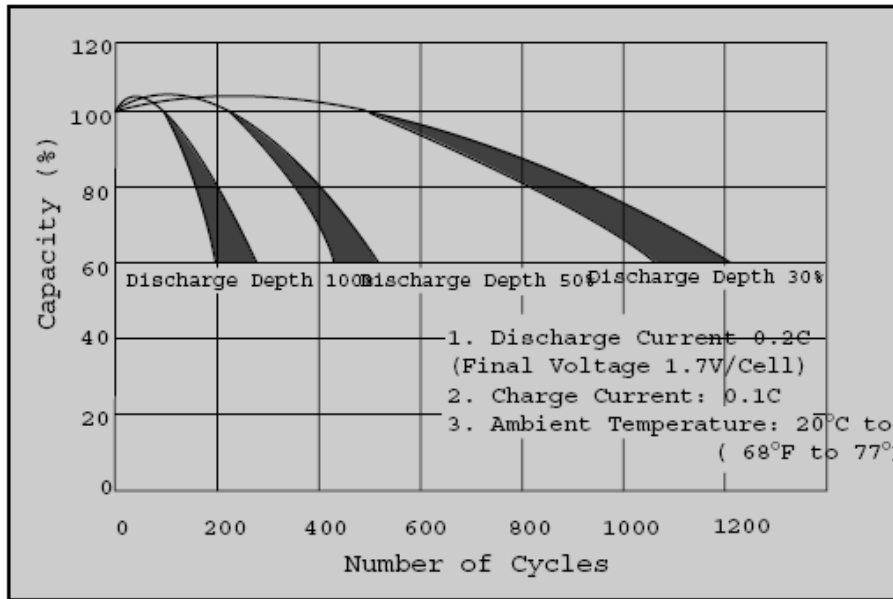


**Figure 2: Depth of Discharge versus battery life [9]**

Typically it should not be greater than  $C/10$ , where  $C$  is the capacity of the SLA battery in Ampere Hours (Ah). A six-cell SLA battery (i.e. 12V nominal voltage) is chosen in the design as it is readily available in the market around the world.

A lead acid battery is very sensitive to temperatures during charging/discharging. In fact, the useful service life is halved for each 10 degree Celsius increase above room temperature [9].

### 4.3 LED Driver

Several semiconductor manufacturers have off-the-shelf WLED driver ICs that can work at high efficiencies with various other features. The major issue encountered with these ICs is that they

only come in surface-mountable packages. Since surface mounting facilities were not readily available, it was decided that the driver circuit be made using prototype-friendly IC packages. Several high efficiency driver designs were considered for the LED driver. A linear converter topology, a low dropout (LDO) current regulator was simulated and built. The simulated LDO converter circuit is shown in figure 3.

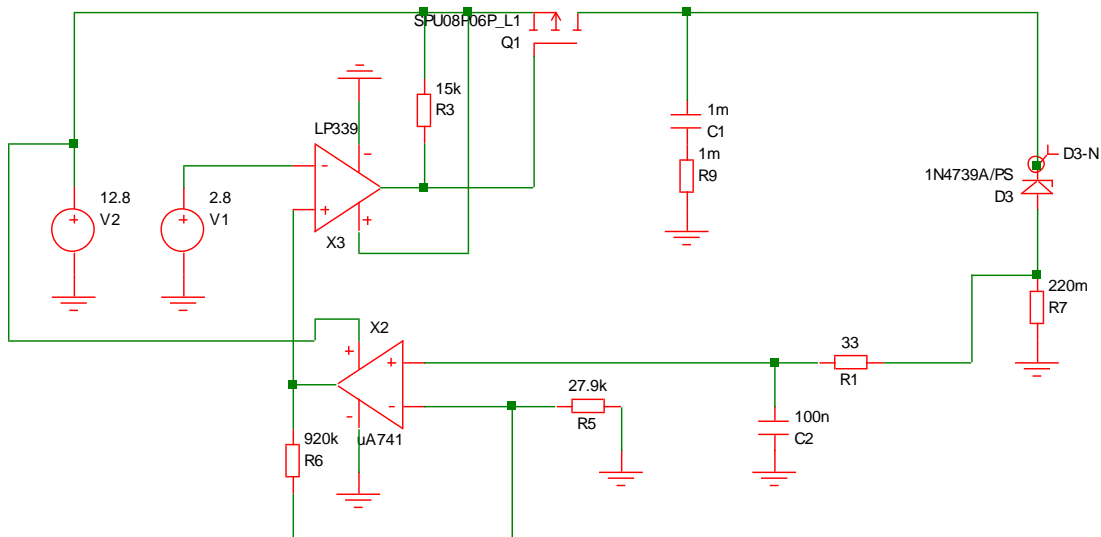


**Figure 3: LDO current regulator**

Here the 9.1V zener diode (D3) represents the voltage drop of three WLEDs.

The advantage of this topology is the simple design requirement of the LDO converter. Another benefit is that no bulky magnetic components such as inductors are needed in a LDO design.

High efficiencies can be achieved with a LDO if the output voltage is close to the input voltage.

When 3 LEDs are driven in series, the output voltage required is about 9.9V (3x3.3V). When a

12V battery is used (of which the terminal voltage is around 12.8V) the voltage difference

between the input and the output is significantly high and thus a high efficiency cannot be

obtained. A highly efficient LDO regulator could be made if a 10V battery was used. Cyclon

batteries from EnerSys can be combined (6V battery and 4V battery in series), to produce 10V.

However, the cost of these batteries was prohibitive and the idea of using a LDO regulator was dropped as a result.

The focus was changed to switch-mode converter topologies and considering its higher efficiency and stability, a current mode buck (step-down) converter topology is employed in the final design. Figure 4 shows the basic building blocks of a buck converter. A buck converter's output voltage is either equal or less than the input voltage. LEDs have a typical forward voltage drop (@350mA current) of about 3.3 ~ 3.5V. Therefore, only 3 LEDs can be connected in series with this configuration (i.e. using a 12V battery). A current sensing resistor is placed in series with the LEDs to sample the current through the LEDs.

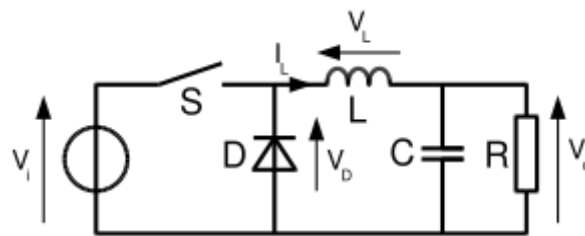


**Figure 4: Components of a buck regulator**

A buck converter as shown in figure 4 suffers from some losses due to the higher forward resistance in diode D. This can be minimized by replacing D with another MOSFET. The improved version is called a synchronous buck converter. However, the higher efficiency comes at the expense of a considerable design complexity. A fault called “shoot-through” can cause the input voltage source to be short circuited if both MOSFETs are turned on at the same time. This should be avoided by adding a time delay to the second MOSFETs gate pulse. Adaptive delay techniques are also available to address this issue [6].

Due to the increased design complexities and time restrictions, a synchronous buck converter was not attempted. The final implementation of the LED driver design is carried out around a current mode PWM IC (UC3843) in association with a buck converter power output stage.

The PWM chip, UC3843 provides the necessary features to implement off-line or DC-DC fixed frequency current mode control schemes with a minimal external parts count. It has a PWM comparator which also provides current limit control [10]. This PWM controller can be operated at a maximum frequency of 500 kHz. At higher frequencies however, switching losses per unit time increases. This is due to the imperfections in the switching waveform such as non-zero rise/fall times, switching spikes etc. Therefore, a low frequency value of 3.6 kHz was chosen for the PWM controller. This does fall within the audio frequency range and does generate some audible noise. However, due to the nature of the application, the audible noise components can be safely ignored.

Another drawback of resorting to a low frequency is that it then requires the magnetic component (i.e. inductor) be large enough to store sufficient amount of energy when the MOSFET is conducting. Since the driver module is outputting currents less than an Ampere, the inductor's current rating does not have to be large. Hence, the actual inductor size can still be kept small.

At the output of the driver stage, the load seen by the circuit is one or two parallel branches of WLEDs, each with three WLEDs connected in series, and a 0.1 Ohm resistor connected in series with the WLED branches.



The purpose of the 0.1 Ohm resistor is to sample the current flowing through the WLEDs by measuring the voltage developed across the resistor. The resistance of this resistor is kept as small as possible to reduce the losses through the resistor. Another strategy to minimize this resistor was to amplify this voltage before presenting to the UC3843 PWM chip as shown in figure 6.

This brings in two advantages:

- 1) The lower resistance helps minimize losses in the converter.
- 2) The maximum current output is easily programmable by changing the gain of the amplifier (OpAmp) section. This allows connecting multiple parallel branches of WLEDs at the output.

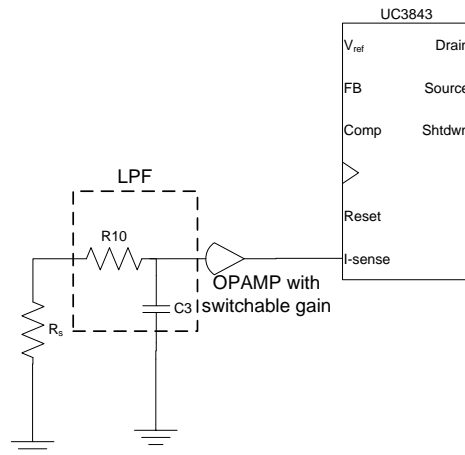


**Figure 6: Amplification of current-sense voltage**

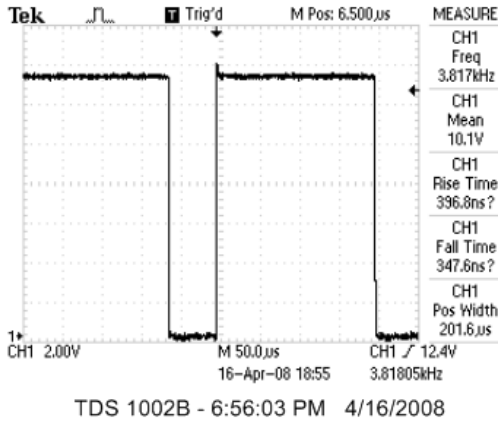
0.1 Ohm is the lowest resistance value that was found to produce reliable and stable operation. A small RC low pass filter (LPF) was used to reduce the switching peak transients in the feedback voltage. The OpAmp's gain is switchable between  $A$  and  $A/2$  where  $A$  is the gain of the OpAmp when only one WLED branch is driven. A DIP switch is used to switch the gain to the desired value on-site, without requiring any hardware changes. This allows the WLED driver module to

be scalable according to the lighting requirements needed at different sites. The power section of the driver consists of typical buck converter. A P-channel MOSFET is used as the power switching device due to its simplicity to be turned on by pulling the gate to ground. Typically, in low to medium power high-side switching application P-channel MOSFETs are used due to this simplicity [11]. Since UC3843's gate drive output is designed to drive an N-channel MOSFET, a MOSFET driver with an inverting output, TC4428 is used to provide the inverted PWM gate pulse. In the buck converter stage, a Schottky diode is used as the freewheeling diode. This reduces the voltage drop across and hence the power dissipation.

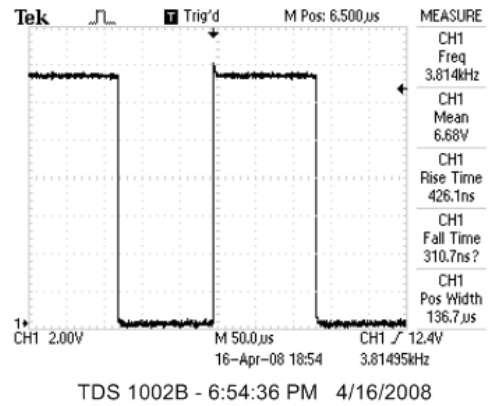
When using two WLED branches, it is assumed that the combined forward voltage of the WLEDs on the secondary branches is approximately equal to that of the primary branch. If binning data for forward voltage is available from the LED manufacturer, it is recommended that closely matched LEDs be used in all the branches (Note: It is observed that not all the manufacturers provide this information; e.g. in an email correspondence, Cree confirmed that they do not currently provide forward voltage binning data for its XLamp XR-E white LEDs. However, Phillips does provide this information for its Luxeon product line).

#### **4.3.1 Soft start**

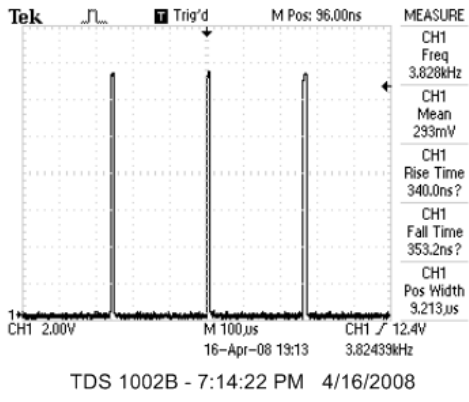
The driver circuit features a soft start mechanism that ensures the initial current through the WLEDs is not exceeding the preset maximum current. This functionality is achieved by charging the capacitor C9 via R6. When power is applied to the UC3843, Q2 turns on as C9 is being charged. Q2's collector is connected to the current sense pin of UC3843 and its voltage rises close to 5V. This minimizes the duty cycle of the gate drive pulse. When C9 is fully charged, current to the base of Q2 is cut-off and Q2 turns off. Now UC3843 can automatically adjust the pulse width according to the pre-set maximum current.



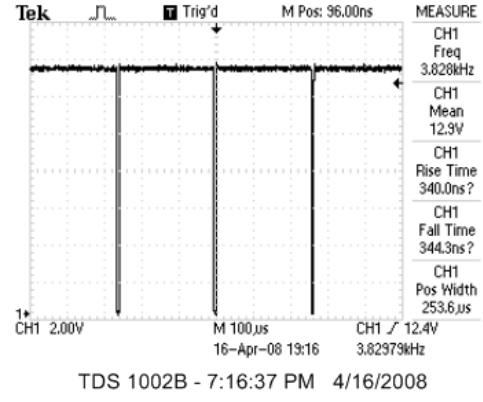
(a)



(b)



(c)



(d)

**Figure 7: WLED Driver MOSFET gate waveforms**

Gate drive waveforms for different scenarios are shown in figure 7. 7(a) shows the gate waveform when only one branch is driven and 7(b) is when two branches are driven. 7(c) is when the output is not connected to any WLED branches and finally 7(d) is when the output is short circuited.

### 4.3.2 Handling WLED failures

If a WLED fails it may fail either as an open circuit failure or a short circuit failure [15]. The driver module is capable of handling any number of failed WLEDs in any failure mode. Since the WLEDs are connected in series (in a branch), the worst case is when all WLEDs have failed

in short circuited mode. Should this happen, the PWM controller minimizes the duty cycle as shown in figure 7(d) and the short circuit current at the output is measured to be 370mA when DIP switch setting is set to two branches and 270mA when DIP switch is set to one branch. The controller circuit could be improved to monitor the voltage across the WLEDs and if it has dropped below the typical forward voltage of a WLED (3.3V @ 350mA), the controller could cut off the power to the PWM controller and an indicator LED could be turned on to warn the maintenance personnel.

**4.3.3 Driver Efficiency**

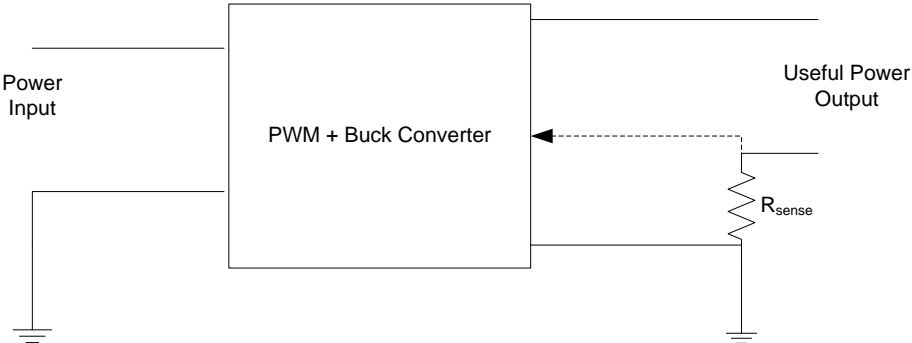


**Figure 8: WLED Driver inputs and outputs**

As seen in figure 8, the output side of the driver is accompanied by a series resistor that is needed by the driver for current regulation. Therefore, a portion of the output power is dissipated in this series resistor. Hence, the actual (useful) power output needs to be considered when calculating the efficiency.

Therefore,

Efficiency of the WLED driver =

$$\frac{\text{Voltage across 3 WLEDs} \times \text{Current through the WLEDs}}{\text{Voltage input to the driver} \times \text{Current drawn by the battery}}$$

	3 LEDs	6 LEDs	
$V_{in}$	13	12.8	V
$I_{in}$	0.34	0.67	A
$V_{WLED}$	9.92	9.84	V
$I_{out}$	0.35	0.71	A
$Power_{in}$	4.42	8.576	W
$Power_{out\_useful}$	3.472	6.9864	W
<b>Useful Efficiency</b>	78.55%	81.46%	

**Table 5: WLED Driver Efficiency Measurements**

Efficiency can be further improved by incorporating a MOSFET with a lower  $R_{DS(on)}$ . Also, modifying the converter architecture to a synchronous buck converter will yield better results in efficiency.

#### 4.4 Controller

The controller was built around a low cost microcontroller chip (PIC 12F675). The features/functions of the controller are therefore customizable through software. The biggest advantage gained by using a microcontroller is its ability to control the long duration on/off timing with reasonable accuracy using only a few lines of code. Currently, the controller is preprogrammed with software that features:

1. Providing a visual indication that the controller is working correctly (i.e. by blinking the lights when powered up initially).
2. Turning on the streetlights when the ambient light intensity drops below 0.2 Lux
3. Turning off the streetlights when the ambient light intensity surpasses 1 Lux.
4. Making sure the battery terminal voltage is always above 12.8V before turning on the lights.
5. Cutting off power to the WLED driver module when the lights have been lit for a pre-determined duration.

6. Making sure the lights are cut-off whenever the battery terminal voltage drops below 12.5V

The main internal microcontroller resources used in this implementation were the ADC (analogue to digital converter) module and the tri-state input/output ports. The PIC 12F675 microcontroller features four ADC input channels, each with 10-bit resolution. The tri-state input/output module has 6 individual ports to accept inputs and output results.

2 out of 4 ADC channels are used in the current version of the software. One ADC channel continuously measures the ambient lighting level and the other ADC channel continuously measures the battery voltage.

As discussed in the system parameter calculations section, the controller should cut off the lights when the battery is 25% discharged. A terminal voltage of 12.5V approximately represents a 25% depth of discharge [14]. In order for the lights to go on, the battery voltage should be at least 12.8V.

The darkness sensitivity is adjusted such that lights are turned on if the ambient illumination is below 0.2 Lux. The lights are cut off when the ambient illumination improves beyond 1 Lux.

#### **4.4.1 Quiescent Power Consumption**

Due to the convenience of prototyping, the WLED driver and the controller modules were built on one PCB. In the current implementation the two modules draw 8mA, which translates into 64mW of power (@12.8V battery voltage). Around 3mA is drawn by the 5V linear regulator (LM78L05) required for the microcontroller. This could be further minimized by using an ultra-low quiescent current voltage regulator such as LM2936 which has a typical bias current of 0.2mA

#### 4.4.2 Minimizing false triggers

False triggers may result in due to invalid analog states at the inputs. For example, birds or other animals may sit right on top of the light detector causing temporary dark conditions that may trigger the lights to go on. On the other hand, at night while the lights are on, weather conditions such as lightening may brighten the skies momentarily causing the lights to go off.

In order to minimize these false triggering due to noisy analog input values and rapid changes, 2-dimensional hysteresis has been implemented in software when acquiring from these analog channels. In one dimension, any analog value in between the lower and upper thresholds is ignored and the current state is maintained. A time lag of 30 seconds is also introduced as the second dimension in that whenever an analog signal large or small enough to make a state change is detected. Therefore, sudden variations are ignored and current state is maintained unless the new ('valid') analog value is maintained for 30 seconds or longer.

The controller and the WLED driver circuits are integrated using an output port on the microcontroller. When it is determined that the lights should go on, fifth tri-state port (GPIO5) is made high. This pin is connected to the non-inverting input of a comparator. The inverting input of the comparator is connected to a voltage between 4V and 5V, so that the comparator output is strictly low, unless otherwise the 'lights on' signal is received from the controller. The output of the comparator is connected to the power pin ( $V_{cc}$ ) of the PWM controller IC (UC3843).

Therefore, the PWM circuit and the power section will only draw current when the lights need to be turned on. This method is useful for saving precious battery energy.

The lowest cost module in the system is the controller module (under \$5.00). This is largely due to the use of a microcontroller. It helps reduce external components and since the logic is built into software, any modification can be made quickly.

### **4.4.3 Software Design**

One of the advantages of using a PIC<sup>®</sup> microcontroller is that it can be programmed in a high level language such as C language and few C compilers are freely available. In this design the C compiler available from Hi Tech Software was used. The program memory of the PIC12F675 is only 1024 words. In the current implementation, only 27.7% of the total program memory is used. While interrupt driven software design generally results in lower power consumption in the microcontroller, a continuous execution loop (without going into SLEEP mode) is employed in the current design. This enables more predictable timing measurements which is more important in this application. The source code is available in Appendix B.

### **4.5 Battery Charger Module**

The useful life of a sealed lead acid battery equally depends on how it is charged as much as how it is discharged. Therefore, it is necessary to charge a SLA battery according to the specifications recommended by the battery manufacturer. It is also desirable to charge the battery in the shortest time possible while adhering to those specifications. Both of these goals can be accomplished by using a specialized lead-acid charger IC. UC3909 is such a product from Texas Instruments. It has separate control loops for both the current and the voltage across the battery for optimal charging control. Since it is a switch mode controller higher efficiencies can be achieved. Charging voltage requirements of a battery vary with the temperature [9]. Therefore, it is vital that the battery temperature is tracked during the charging process. The UC3909 does monitor the battery temperature (via an external thermistor attached to the battery) and adjusts the charge voltage accordingly. UC3909 provides a 4-state charging process. The initial charging state is called the trickle charge mode where only a low current is passed through the battery until it reaches a threshold voltage. Since this charging mode makes the charging process take a

longer time to reach the regular charging mode, trickle charge mode is not normally used in cyclic application and limited to stand by applications. Therefore, in this implementation, a three-state lead-acid battery charger was implemented by disabling the initial trickle charge mode. Same as the WLED driver module, a buck DC-DC converter is employed at the output stage of the charger to achieve high efficiencies.

The charger's parameters were calculated based on the application note in [17]. The prototype of the battery charger is designed to charge a 28Ah battery. However, it can easily be switched to properly charge a 12Ah battery by changing one resistor (R4) to 4.7k $\Omega$ . R4 is the resistor that determines the overcharge-terminate current. By switching to 4.7k $\Omega$ , this current threshold can be lowered to about 250mA. It matches with a smaller (13Ah) battery and a proper full charge can be expected as a result. This can be built right into the prototype so that the correct resistor value is selected via a DIP switch based on the desired configuration.

#### **4.5.1 Charging Algorithm**

Whenever sufficient sunlight is available so that the PV panel can generate a voltage greater than that of battery's, the charger begins charging the battery.

#### **4.5.2 Bulk Charge Mode**

In this mode the current through the battery is maintained constant. This current should not exceed 0.2xC Ampers [9]. The battery capacity needed for the two-branch and one-brach configurations is 28Ah and 13Ah respectively and based on its specifications, a 30W PV panel (used in the two-branch configuration) can supply only up to 1.78A. Therefore, bulk current was set to 2A so that it is safe even for the 13Ah battery. Bulk charge mode replenishes 70% to 90% of the battery capacity [16].

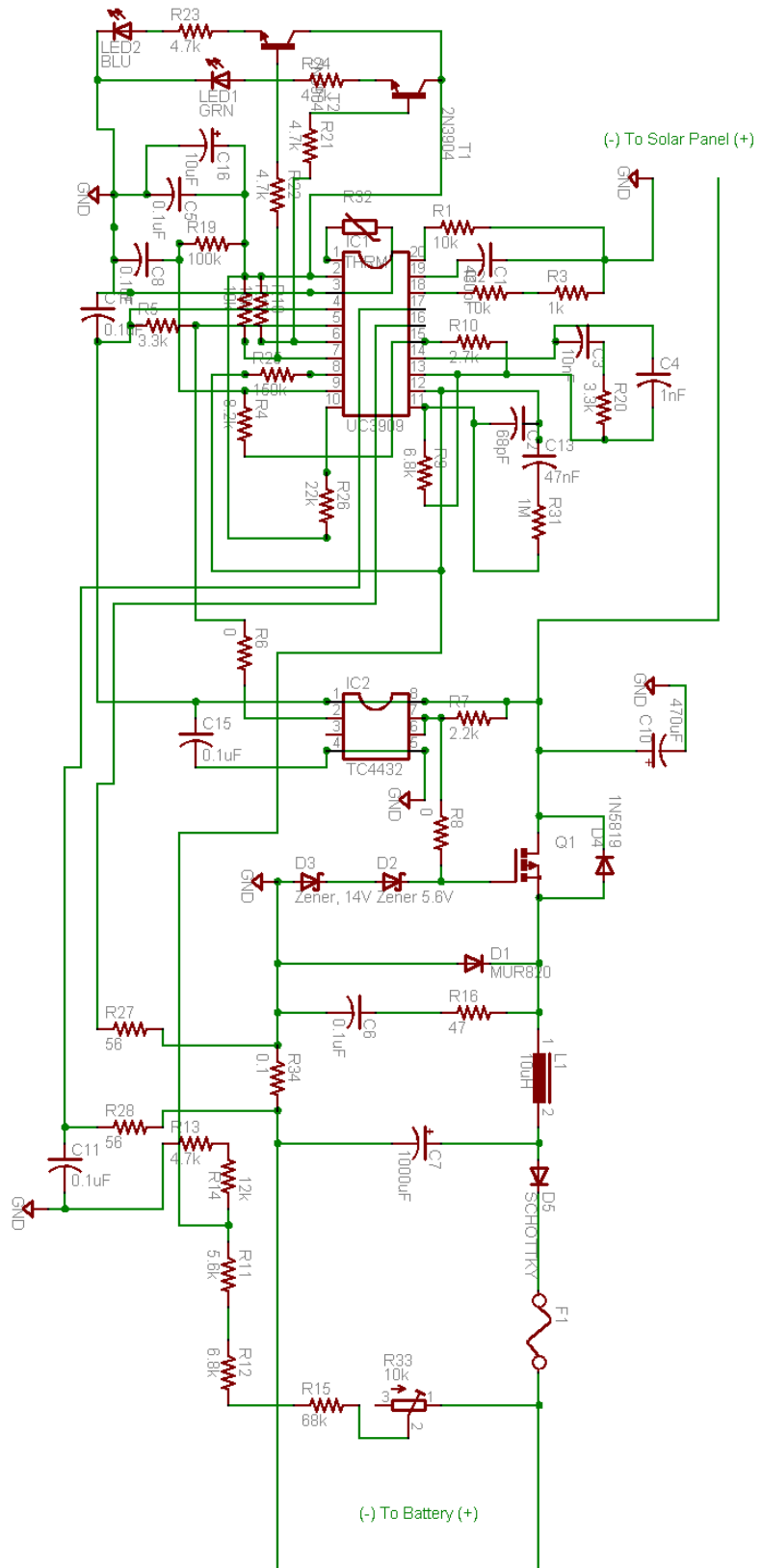
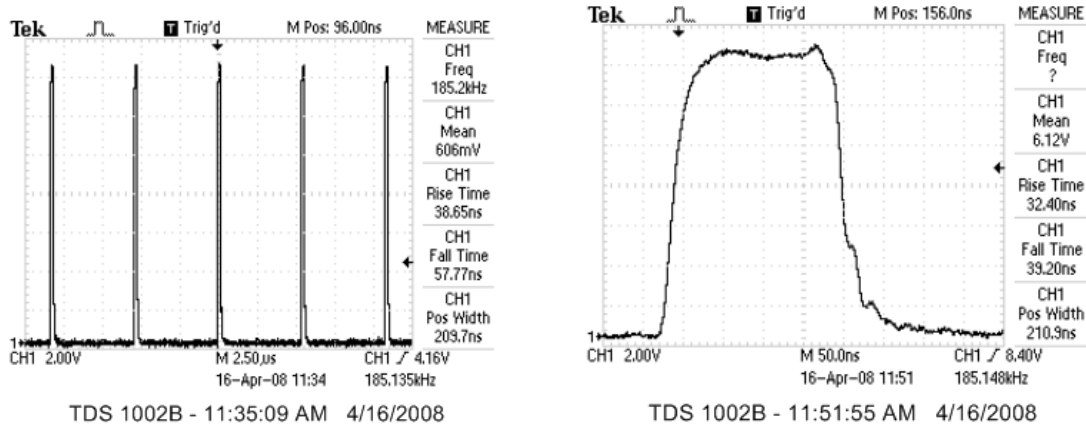


Figure 9: Battery Charger Schematic

On the prototype, the bulk mode is indicated by the blue indicator LED. Figure 10 shows the gate waveforms in the during the bulk charge mode. The waveform to the right is the zoomed in view of the left waveform.



**Figure 10: Bulk charge mode – MOSFET gate waveforms**

#### 4.5.3 Overcharge Mode

As the battery voltage increases, it reaches a pre-set threshold voltage (13.9V, @25 degree Celsius) at which point the blue LED turns off and green LED turns on indicating it entered the overcharge state. At the beginning of this mode, the same current level as in the bulk mode is supplied to the battery. When the battery voltage reaches a preset overcharge voltage level (14.8V, @ 25 degree Celsius) the current begins to taper off and the control is transitioned from current limiting to voltage limiting mode. The oscilloscope traces shown in figure 11 show the gate drive of the MOSFET at the beginning of the overcharge mode (left) and towards the end of the overcharge mode (right).

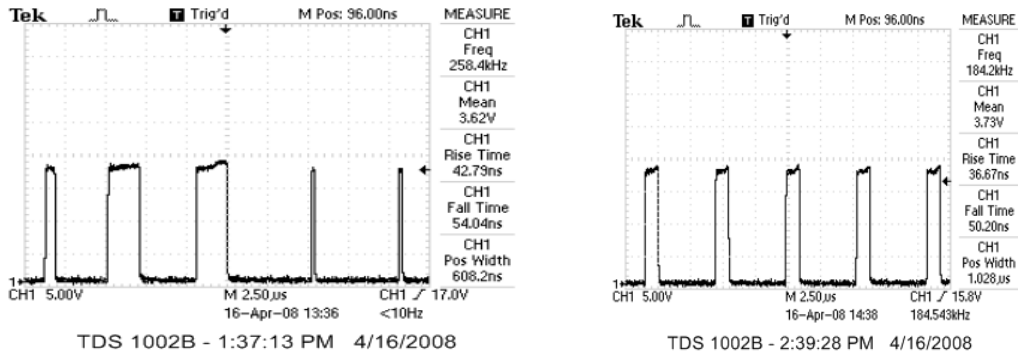


**Figure 11: Over charge mode – MOSFET gate waveforms**

#### 4.5.4 Float Charge Mode

When the charge current is tapered to a preset current threshold (usually  $0.2 \times$  Bulk current; i.e. 400mA, approximately), it switches to the float charge mode, in which the battery voltage is maintained at a constant level. This voltage is usually 2.25V per cell (i.e. 13.5V). When the battery charger switches to the float charge mode, it is indicated by turning on both the green and blue LEDs. Reaching the float charge mode also means that the battery is fully charged.

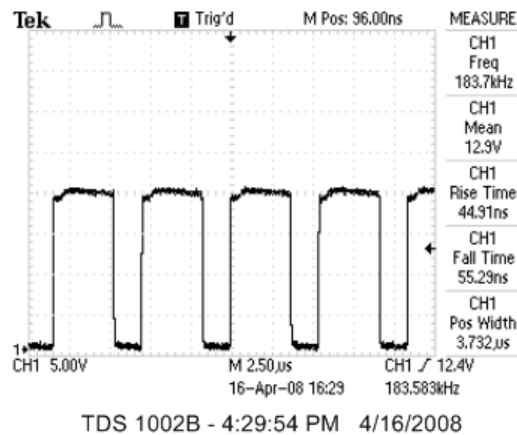


**Figure 12: Float charge mode – MOSFET gate waveform**

#### 4.5.5 Battery Charger Efficiency

Unlike the WLED driver, battery charger’s input/output voltages/currents vary significantly over the course of the complete charge cycle. Therefore, efficiency calculations were made during

each charge mode and presented separately. Also, an average calculation is made using these measurements. Following the same argument with the WLED driver efficiency, the actual (useful) efficiency values are presented here. Based on the three measurements, the average efficiency is calculated to be 81.98%

	<b>Bulk</b>	<b>Over Charge</b>	<b>Float</b>
$V_{in}$	14.54 V	15.17 V	18.96 V
$I_{in}$	1.74 A	1.74 A	0.21 A
$V_{bat}$	13.31 V	13.86 V	13.54 V
$I_{out}$	1.725 A	1.725 A	0.19 A
$P_{in}$	25.30 W	26.3958	3.98 W
$P_{out\_useful}$	22.96 W	23.9085	2.57 W
<b>Useful Efficiency=</b>	<b>90.75%</b>	<b>90.58%</b>	<b>64.61%</b>

**Table 6: Battery Charger Efficiencies**

#### 4.5.6 Battery Protection

Two protection mechanisms are employed to protect the battery from being discharged through the charger and protection against polarity reversal. The former is achieved with a Schottky barrier diode connected in series with the battery. When the battery charger's voltage is lower than the battery's voltage, this diode is reverse biased and battery is isolated from the charger circuit. In case of an incorrect connection of the battery, current will flow through the freewheeling diode, the inductor and the Schottky diode back into the battery. The fuse in series with the battery will then break and the battery is protected against being short circuited permanently.

#### 4.6 White Light Emitting Diodes (WLED)

High brightness white light emitting diodes are employed at the output stage. LEDs are efficient and long lasting. The use of *white* LEDs are because of their beneficial natural light characteristics. As of now, commercially available WLEDs can produce up to 107 lumens at forward drive current of 350mA. (e.g. Cree XLamp 7090 XR-E white LED) at a forward diode

current of 350mA. It was noted that manufacturer's claims on luminous flux is rated at a junction temperature of 25 degree Celsius. Therefore, the practical value for the luminous flux is less than this value as the operational junction temperature will be higher than 25C.

Since LEDs are very sensitive to current variations, current through these LEDs is tightly regulated. Power LEDs do produce some heat which should be carried away efficiently from the LED chips using heat sinks in order to maintain the junction temperature at a prescribed value. The WLEDs used (Cree XLamp XR-E) were already mounted on a metal core printed circuit board (MCPCB). To ensure thermal stability and longer life, external heat sinks were mounted to the back of the WLEDs.

#### 4.6.1 Thermal Calculations

The thermal resistance from junction to solder point ( $R_{th\ j-sp}$ ) is listed in the data sheet as 8°C/W.

The maximum LED junction temperature ( $T_j$ ) provided in the data sheet is 145°C.

Therefore,

$$T_j = T_{ambient} + P_{total} (R_{th\ j-sp}/6 + R_{th\ sp-h}/6 + R_{th\ h-a})$$

The thermal-resistance between the LED solder point and the heat sink,  $R_{th\ sp-h}$ , depends on the surface finish, flatness, applied mounting pressure, contact area, and the type of interface material and its thickness and can be minimized to less than 1°C/W. The maximum thermal resistance from the heat sink to ambient ( $R_{th\ h-a}$ ) can thus be calculated.

In order to meet the manufacturer's rated lamp life of 50, 000 Hrs (at which point lumen maintenance is 70%) WLEDs should be operated at a junction temperature of 85°C or below [8].

Therefore, when selecting a heat sink, the target junction temperature was selected to be 85°C.

$$R_{th\ h-a} = (85^\circ\text{C} - 35^\circ\text{C} - 8^\circ\text{C}/\text{W} \times 1.155 \times 6/6 - (1^\circ\text{C}/\text{W} + 0.8^\circ\text{C}/\text{W for the thermal adhesive}) \times 1.155 \times 6/6) \text{ W} = 38.68^\circ\text{C}/\text{W}$$

## 4.7 Optical Modifiers

Due to the nature of the application, it is important that light be efficiently directed to where it is most needed. A street in general, is a strip of land. In order to illuminate the street efficiently, light output from the lamps should be guided along this strip with a minimum amount of ‘spill’. Out of the box, LEDs do not have an illumination pattern that meets this requirement. Therefore, optical modifiers or lenses are required for this purpose. A suitable lens is available from an LED optics maker – L2Optics. This lens is called the “flare lens”. It has a very narrow illumination distribution along one axis and a very wide light distribution on the other axis. This closely represents the spatial characteristics of a street. Currently, these lenses are only manufactured for Lumileds’ Luxeon LEDs.

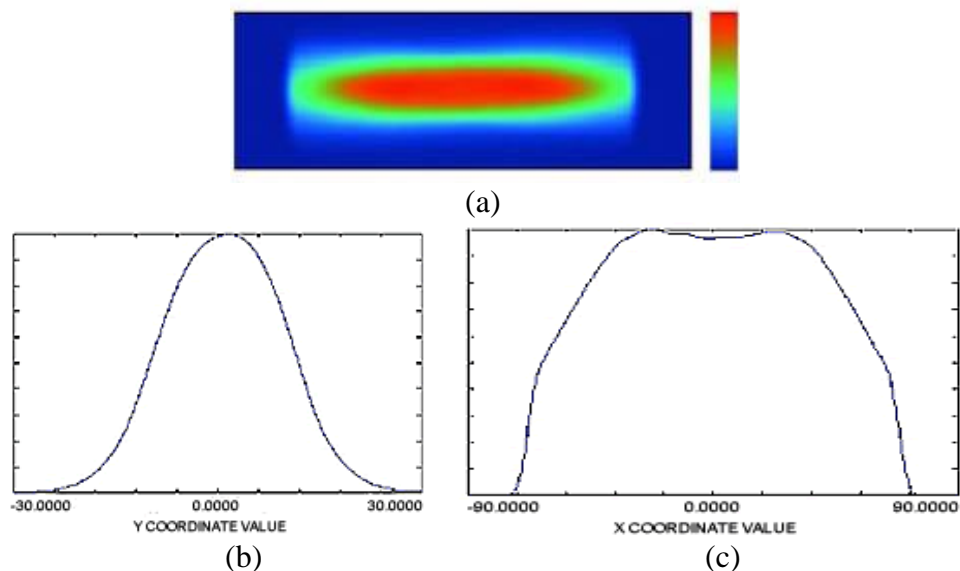


**Figure 13: Light Distribution Characteristics of Flare Lens by L2Optics**

Figure 13(a) illustrates a typical illumination pattern of the flare lens and according to Figure 13(b) and 13(c) the half angle divergence of the lens has a typical vertical distribution of  $\pm 10^\circ$  and a typical horizontal distribution of  $\pm 80^\circ$  respectively [18]. According to the manufacturer’s specifications, this lens has a minimum optical efficiency of 85%.

It was observed, however, the actual light output efficiency was much higher than 85%. When one LED branch was driven at 350mA, the light output was 294 lumens. With the lenses, it only reduced to 270 lumens. This translates into an optical efficiency of 91%.

#### **4.8 Luminaire/Lamp Post**

In the current implementation, only parts of the luminaire and the post were finished. The LEDs were attached to the inside of the luminaire by screwing bolts into the heat sinks. Currently, no outside cover is used. A transparent and hard plastic (e.g. Polymethyl methacrylate – PMMA) material is appropriate for this purpose. It might be possible to design this cover such that the lamp lenses will be exposed to outside. The benefit of this approach is that the overall (optical) efficiency would be higher if the lenses were exposed. However, in the long run, there is a higher probability of accumulating dust and grime on the lenses as they have uneven surfaces (bumps and dips) as opposed to a smooth/flat surface offered by a luminaire cover. Therefore, the overall efficiency may still go down with time and this efficiency can be brought up to the original level at an additional regular maintenance expense.

The lamp post would need to be made of a rugged material (e.g. treated wood, stainless-steel, or aluminum). It is believed that the availability and the local economics may govern the final selection. The lamp post will also house the battery and the circuitry. The housing will have to be weather-proof and sturdy enough to carry the weight of the battery (around 25 pounds for a 35Ah SLA battery). The solar PV panel will also be mounted on top of the post facing the sun. The PV panel's connecting arm to the pole should be adjustable along both horizontal and vertical axes so that its surface is positioned to receive the maximum amount of sunlight available. Another boom pole connected to the lamp post houses the luminaire fixture.

## **Chapter Five - System Scalability and Adaptability**

The lighting needs of different deployments may also be different. Therefore, scalability and adaptability is a main design feature addressed when designing the system. This system is capable of scaling down by a factor of two without any hardware modifications.

High brightness LEDs are rapidly being improved in many aspects. The newer LED technologies offer more light output per one Watt over a longer service life. As long as those LEDs can be driven at @350mA, this design can accommodate future LED technologies with virtually no changes.

Also, several parameters in the design are allowed to be varied based on the deployment requirements. This feature allows the system to adapt to conditions at the site, without core design modifications. The parameters that can be varied are:

- Total lumen output per installation
- Illumination distribution

### **5.1 Total Lumen Output**

This system can accommodate either 6 or 3 WLEDs. If only 3 WLEDs are installed, the battery and the PV panel can be halved in capacity. On the WLED driver circuit, the DIP switch 4 should be set to ON position when driving 3 WLEDs.

Alternatively, if the system is fitted with 6 WLEDs, the DIP switch 4 should be left at OFF position. In either case, each 3-WLED branch is driven at 350mA.

### **5.2 Illumination distribution**

Spatial illumination distribution is a function of lens orientation. Therefore, by placing the same lenses strategically, different illumination patterns can be achieved. Figure 14(a) illustrates

placing of 6 lenses with the same orientation. With flare lenses, this would result in a wider beam distribution along Y axis and a narrower beam distribution along X axis. This would be appropriate for lighting a street. By rotating the orientation of 3 lenses by 90° degrees, as shown in Figure 14(b), wider distributions along both X and Y axes can be accomplished. This configuration would be more suitable for lighting up an intersection or a common area in a refugee camps etc. However, the illumination level will be cut in half in each direction as only three lights are used per axis. This can be minimized by driving the lamps at a higher current which will yield a higher luminous output. Although, the drawback of this approach is that the efficacy of the LEDs is reduced with increasing driving current and the service life may be degraded unless the junction temperature is kept below 85°C.

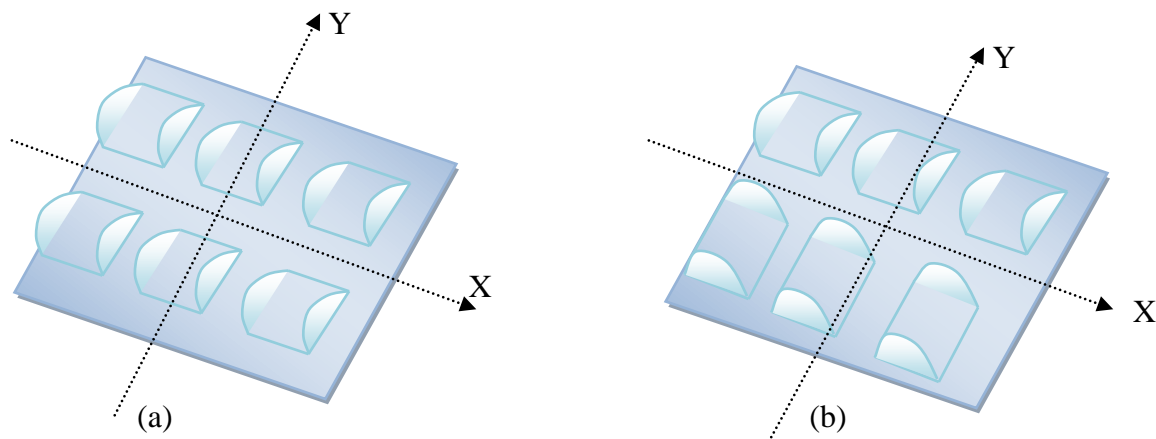


**Figure 14: Spatial Illumination Distribution and Lens Orientation**

## Chapter Six - Cost Analysis

The capital cost breakdown is shown in table 7 for the two possible configurations.

	3 WLEDs	6 WLEDs
<b>Solar PV</b>	\$75.00	\$150.00
<b>Battery</b>	\$45.00	\$90.00
<b>Battery charger</b>	\$19.68	\$19.68
<b>Controller</b>	\$4.40	\$4.40
<b>WLED Driver</b>	\$11.44	\$11.44
<b>WLEDs</b>	\$42.21	\$84.42
<b>Pole + Mounting hardware</b>	\$50.00	\$50.00
<b>Capital Cost =</b>	\$247.74	\$409.95

**Table 7: Capital Cost Breakdown**

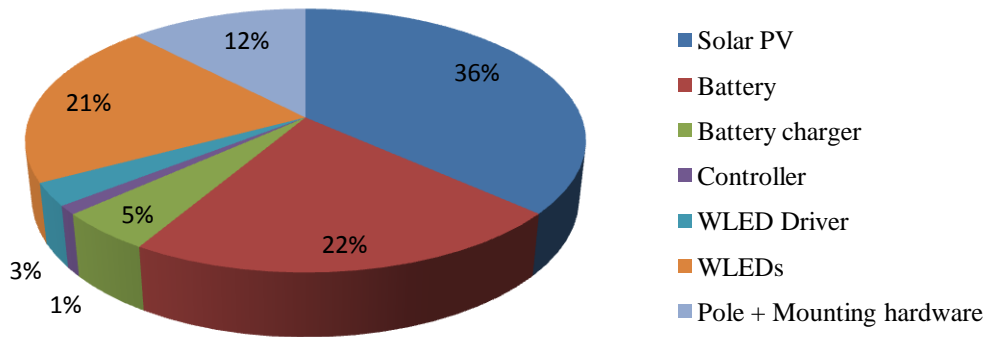


**Table 8: Capital Cost Breakdown for 6 WLEDs**

However, capital cost alone does not provide any information about the operational life of different components of the system. Life cycle cost (LCC) analysis on the other hand, takes into account the potential costs expected during the life of an item over some finite period. An annualized life cycle cost (ALCC) is also calculated in this analysis. Essentially, ALCC is the

total LCC expressed as an yearly cost. ALCC is a more useful parameter to the user as it provides a measure of yearly expense towards the system rather than being presented with the ‘total’ cost over the life span of the product which may be difficult to justify.

The following assumptions are made for this analysis:

Discounting factor	=	10%
Inflation rate	=	0
Battery is replaced at every	=	3 years
Duration considered for analysis	=	10 years

### 6.1 LCC and ALCC for One WLED branch

<b><u>Capital Costs</u></b>			
Solar PV	\$	75.00	
Battery	\$	45.00	
Battery charger	\$	19.68	
Controller	\$	4.40	
WLED Driver	\$	11.44	
WLEDs	\$	42.21	
Pole + Mounting hardware	\$	50.00	
<b>Capital Cost =</b>			<b>\$ 247.74</b>
<b><u>Replacement Costs</u></b>			
Battery at			\$ 40.00
	at year	Pr factor	PW
	3	0.75	\$ 30.00
	6	0.56	\$ 22.40
	9	0.42	\$ 16.80
<b>Net Present Worth of Replacements</b>			<b>\$ 69.20</b>
<b>Total Life Cycle cost</b>			<b>\$ 316.94</b>
factor Pa over 10 years			6.14
<b>Annualized cost</b>			<b>\$ 51.62</b>

## 6.2 LCC and ALCC for Two WLED Branches

<b><u>Capital Costs</u></b>			
Solar PV		\$	150.00
Battery		\$	90.00
Battery charger		\$	19.68
Controller		\$	4.40
WLED Driver		\$	11.44
WLEDs		\$	84.42
Pole + Mounting hardware		\$	50.00
<b>Capital Cost =</b>		<b>\$</b>	<b>409.95</b>
<b><u>Replacement Costs</u></b>			
Battery at		\$	90.00
			PW
	at year	Pr factor	
	3	0.75	\$ 67.50
	6	0.56	\$ 50.40
	9	0.42	\$ 37.80
<b>Net Present Worth of Replacements</b>		<b>\$</b>	<b>155.70</b>
<b>Total Life Cycle cost</b>		<b>\$</b>	<b>565.65</b>
factor Pa over 10 years			6.14
<b>Annualized cost</b>		<b>\$</b>	<b>92.13</b>

Some recurring maintenance costs may be applicable for both the cases but those costs are ignored for simplicity. The second largest capital expense, the rechargeable battery's cost used in the analysis is the cost of a single battery. Therefore, it may be possible to reduce the capital expenses and the replacement costs if these batteries can be sourced in bulk quantities for a lower price.

## Chapter Seven - Field Measurements

The prototype of the street lamp and the lamp post was tested outdoors and the performance measured. The location chosen for this purpose was an empty parcel of land in the Research Park area of the University of Calgary campus.



**Figure 15: Digital photos of the street lamp during the field measurements**

The land itself was unlit by any artificial lighting source. However, the clear skies with a bright moon approaching full moon (about 95% full-moon), the ambient light was noticeable but variable from point to point. The distant pathway lights and the surrounding trees may be

accountable for this variation. It was decided to take two sets of measurements with the street light turned off and the street light turned on. The illuminance measurement without the light is the ambient Lux level. This value is subtracted from the Lux measurement taken with the light turned on. In order to minimize the error due to background light, both WLED branches were turned on to get the maximum light output possible. The measurement data is available in Appendix C.

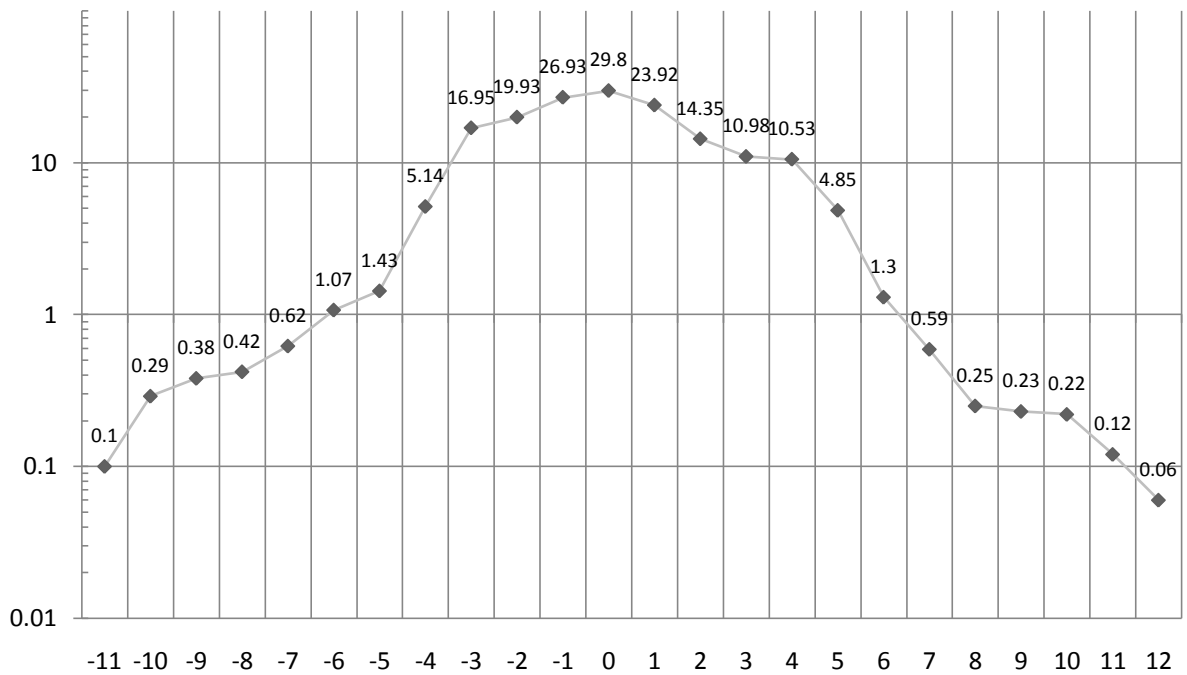


**Figure 16: Vertical Illuminance distribution (Lux) vs. the distance along the street (m)**

The strip of land lit by the street light is clearly seen in the photos in figure 15. The advantage of the high CRI of the WLEDs is clearly observed in that the natural colors are well reproduced when lit by this lamp. The bottom shot shows the difference of color reproduction between the WLED street light and the regular sodium vapor street lights (in the background).

According to the graph in figure 16, the target illumination level is achieved at an approximate linear distance of 12m from the lamp post. This indicates that by installing lamp posts at twice

this distance, i.e. at 24m (78 feet), the target illuminance of 0.1 Lux is achievable. According to the data shown in figure 17, there is enough illuminance to light up a street about 7m wide. There is a rapid decay of illuminance to the back of the lamp post. This is a result of the angle (approx. 100° with the horizontal plane) at which the boom is fixed.

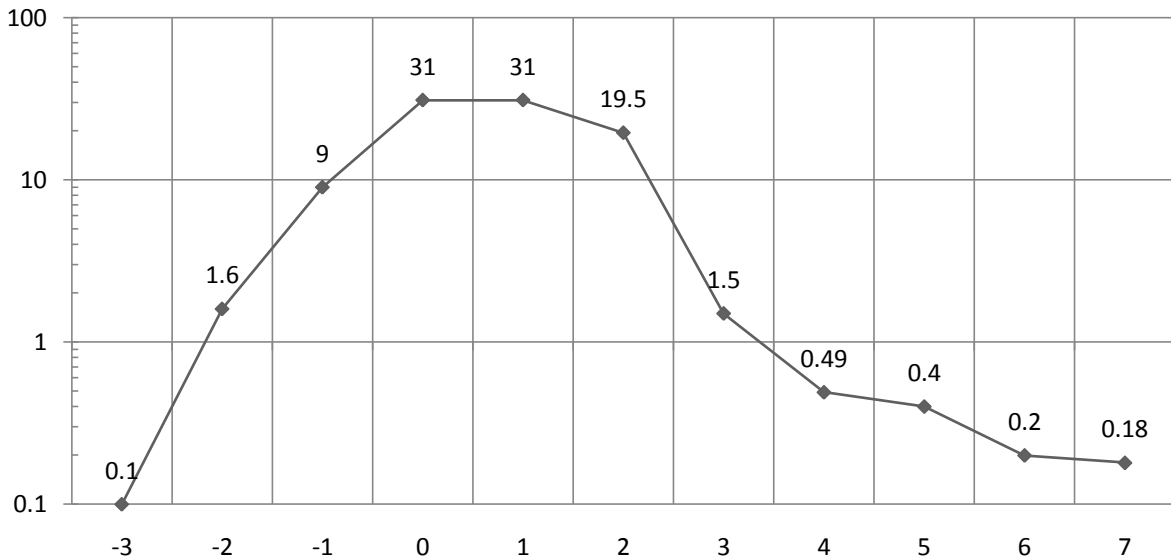


**Figure 17: Vertical Illuminance distribution (Lux) vs. the distance across the street (m)**

The maximum vertical illumination measurement recorded (right underneath the lamp) was 31 Lux. For comparison, another measurement was taken underneath a pathway street lamp (HPS) of which the post height was 25 feet. The maximum illuminance measurement obtained was 44 Lux.

## Chapter Eight - Conclusion and Future work

In this project, a prototype of a solid state street light was designed, built and tested. The modular design approach helped build a system that is easily scalable. The light output of the system (with two WLED branches) is sufficient to light up a street when 15 feet lamp posts are placed 78 feet apart from each other.

In this first iteration, some of the features were not implemented. The following are some of the work planned to be completed in the future.

- 1) In the current design, light output level is kept constant throughout the running time. This can be improved so that the light output can be varied depending on the time of the day. Assuming low usage around midnight hours, light output can be reduced during these hours so that the total running time can be extended with the system running at full power during busy evenings and morning hours. A manual override can be supplied so that the system can switch to full power upon user's command.
- 2) In this version of the system, the days of autonomy (i.e. the number of days of service without sufficient sunlight to recharge the battery) is loosely defined. If sunlight is not received for an extended period of time, the system will continue to run the lighting cycle as long as the battery terminal voltage does not go lower than the preset cut off value. In order to define the days of autonomy more accurately, system design should be modified so that on any regular day, the PV panel can generate sufficient power to replenish the battery that may have been drained for 'n' number of days continuously. It should be noted, however, this can result in higher cost as the battery and the PV panel should be larger in capacity to handle the extra load.

- 3) The lamp post is not fully designed yet. The lamp post should have another arm built to mount the PV panel. Also, the post should have another enclosure to house all the electronics and the battery.
- 4) The luminaire also needs more work. The WLEDs should be put in a weather-proof enclosure. The lenses can be exposed to outside as discussed in 4.8
- 5) The battery charger module's PCB does not currently provide an option to switch between a one-branch and two-branch system (to charge either a 28Ah or 13Ah battery). A DIP switch should be installed to switch the resistor. More details are available in 4.5
- 6) The controller should be built with a separate indicator LED to show the battery status. When the battery reaches its end-of-life, it can be identified easily with a dedicated indicator. The controller can determine if the battery has come to its end-of-life by monitoring if it is required to turn off the lamps prematurely over consecutive cycles due to battery voltage being dropped below the cut off threshold before the running time is complete.
- 7) Currently the battery charger is operating completely separate from the controller module. If the controller has knowledge of how much power the battery charger was able to pump into the battery, it can more accurately decide how long the battery can supply energy for the following lighting cycle. This added intelligence can be fed to the controller by having it monitor the battery voltage and the charging current during the charging cycle using the ADC inputs. An algorithm to calculate the power transferred to the battery can be written in the controller's software.

## Appendix A - Component list and pricing

<b>WLED Driver</b>			
<b>Part</b>	<b>Value</b>	<b>Cost (unit cost when purchasing 100)</b>	
<b>C1</b>	0.1uF	\$	0.09
<b>C2</b>	0.047uF	\$	0.09
<b>C3</b>	0.1uF	\$	0.09
<b>C4</b>	0.1uF	\$	0.09
<b>C5</b>	100uF	\$	0.07
<b>C6</b>	0.1uF	\$	0.09
<b>C7</b>	470uF	\$	0.61
<b>C8</b>	.1uF	\$	0.09
<b>C9</b>	4.7uF	\$	0.07
<b>C12</b>	0.1uF	\$	0.09
<b>D1</b>	MUR 160	\$	0.25
<b>F1</b>	FUSE	\$	0.20
<b>IC1</b>	LMC662CN	\$	1.15
<b>IC2</b>	UC3843	\$	1.26
<b>IC3</b>	TC4428	\$	0.90
<b>L1</b>	47uH	\$	0.92
<b>Q1</b>	SPP08P06P MOSFET	\$	2.71
<b>HS</b>	MOSFET Heatsink	\$	0.41
<b>Q2</b>	2N3906	\$	0.06
<b>R1</b>	220k	\$	0.02
<b>R2</b>	10k	\$	0.02
<b>R3</b>	100k	\$	0.02
<b>R4</b>	47	\$	0.02
<b>R5</b>	10k	\$	0.02
<b>R6</b>	220k	\$	0.02
<b>R7</b>	27k	\$	0.02
<b>R8</b>	47k	\$	0.02
<b>R9</b>	0.1, 2W	\$	1.47
<b>R10</b>	33	\$	0.02
<b>S1</b>	DIP SWITCH	\$	0.53
<b>Total cost</b>		<b>\$</b>	<b>11.44</b>

<b>Controller</b>			
<b>IC4</b>	PIC12C672P	\$	1.03
<b>IC5</b>	78L05Z	\$	0.41
<b>C11</b>	10uF	\$	0.05
<b>R12</b>	27k	\$	0.02
<b>R13</b>	LDR	\$	1.02
<b>R11</b>	10k	\$	1.50
<b>C10</b>	0.1uF	\$	0.09
<b>R16</b>	3.3k	\$	0.02
<b>R14</b>	6.8k	\$	0.05
<b>R15</b>	3.3k	\$	0.02
<b>LED1</b>	LED5MM	\$	0.14
<b>Total</b>		<b>\$</b>	<b>4.40</b>

<b>WLEDs + Lens + Heat Sink</b>			
<b>D2</b>	Cree XLamp	\$	10.00
<b>D3</b>	Cree XLamp	\$	10.00
<b>D4</b>	Cree XLamp	\$	10.00
<b>D5</b>	Cree XLamp	\$	10.00
<b>D6</b>	Cree XLamp	\$	10.00
<b>D7</b>	Cree XLamp	\$	10.00
<b>HS</b>	WLED Heatsink (QTY. 6)	\$	6.42
<b>LENS</b>	QTY.6	\$	18.00
<b>Total</b>		<b>\$</b>	<b>84.42</b>

<b>Battery Charger</b>			
<b>Part</b>	<b>Value</b>	<b>Cost (unit cost when purchasing 100)</b>	
<b>C1</b>	430pF	\$	0.09
<b>C2</b>	68pF	\$	0.09
<b>C3</b>	10nF	\$	0.09
<b>C4</b>	1nF	\$	0.09
<b>C5</b>	0.1uF	\$	0.09
<b>C6</b>	0.1uF	\$	0.09
<b>C7</b>	1000uF	\$	0.61
<b>C8</b>	0.1uF	\$	0.09

<b>C10</b>	470uF	\$	0.61
<b>C11</b>	0.1uF	\$	0.09
<b>C13</b>	47nF	\$	0.09
<b>C14</b>	0.1uF	\$	0.09
<b>C15</b>	0.1uF	\$	0.09
<b>C16</b>	10uF	\$	0.07
<b>D1</b>	MUR820	\$	0.25
<b>D2</b>	Zener, 5.6V	\$	0.34
<b>D3</b>	Zener, 14V	\$	0.34
<b>D4</b>	1N5819	\$	0.25
<b>D5</b>	SCHOTTKY 5A	\$	0.89
<b>F1</b>	Fuse	\$	0.20
<b>IC1</b>	UC3909	\$	4.44
<b>IC2</b>	TC4432	\$	2.15
<b>L1</b>	10uH	\$	0.92
<b>LED1</b>	GRN	\$	0.14
<b>LED2</b>	BLU	\$	0.14
<b>Q1</b>	SPP08P06P MOSFET	\$	2.71
<b>HS</b>	MOSFET Heatsink	\$	0.41
<b>R1</b>	10k	\$	0.02
<b>R2</b>	10k	\$	0.02
<b>R3</b>	1k	\$	0.02
<b>R4</b>	8.2k	\$	0.05
<b>R5</b>	3.3k	\$	0.02
<b>R7</b>	2.2k	\$	0.02
<b>R9</b>	6.8k	\$	0.05
<b>R10</b>	2.7k	\$	0.05
<b>R11</b>	5.6k	\$	0.05
<b>R12</b>	6.8k	\$	0.05
<b>R13</b>	4.7k	\$	0.05
<b>R14</b>	12k	\$	0.05
<b>R15</b>	68k	\$	0.05
<b>R16</b>	47	\$	0.02
<b>R17</b>	10k	\$	0.02
<b>R18</b>	10k	\$	0.02
<b>R19</b>	100k	\$	0.02
<b>R20</b>	3.3k	\$	0.02
<b>R21</b>	4.7k	\$	0.02
<b>R22</b>	4.7k	\$	0.02
<b>R23</b>	4.7k	\$	0.02
<b>R24</b>	4.7k	\$	0.02

<b>R25</b>	150k	\$	0.05
<b>R26</b>	22k	\$	0.02
<b>R27</b>	56	\$	0.02
<b>R28</b>	56	\$	0.02
<b>R31</b>	1M	\$	0.02
<b>R32</b>	THRM	\$	0.29
<b>R33</b>	10k	\$	1.50
<b>R34</b>	0.1, 2W	\$	1.47
<b>T1</b>	2N3904	\$	0.06
<b>T2</b>	2N3904	\$	0.06
<b>Total Cost</b>		<b>\$</b>	<b>19.68</b>

## Appendix B - C language source code for PIC12F675 microcontroller

```
#include "pic.h"
#include "delay.h" //available with Hi Tech C compiler
#include "math.h"

const unsigned int cBatHiThresh = 854;//represents 12.8V at the battery
const unsigned int cBatLoThresh = 834;//represents 12.5V at the battery
const unsigned int cDarkHiThresh = 926;//represents darkness level to activate lights 0.2Lux
const unsigned int cDarkLoThresh = 723;//represents enough darkness level to turn off lights 1Lux
const unsigned int cDurationInSeconds = 10*3600; //represents the maximum uptime for lamps in
seconds. Currently running time is 10 hours
const unsigned int cResponseDelayInSeconds = 5; //delay introduced before alternating between the
lights ON/OFF states

void wait_seconds(int secs)
{
    unsigned int j;
    for(j=0;j<4*secs;j++) //wait a second
        DelayMs(250);
}

unsigned int uiADC(char cSource)
{
    unsigned int uiAnalog=0;
    switch (cSource)
    {
        case 'B': ADCON0 = 0b10000001; ANSEL = 0b000100001; break; //input is AN0
        case 'L': ADCON0 = 0b10000101; ANSEL = 0b000100010; break; //input is AN1
    }
    ADCON0 = (ADCON0 | 0b00000010); //Start AD conversion
    while((ADCON0 & 0b00000010) !=0); //Check for end of conversion

    uiAnalog = (ADRESH<<8) | ADRESL;
    return uiAnalog;
}

void init(void)
{
    short i;
    TRISIO = 0b000011; // set GP0 & GP1 as inputs and others as output
    CMCON = 0b00000111; //comparator OFF
    GPIO5 = 0; //make sure the lights are turned off at boot up.
    wait_seconds(2); // two-second initial delay
    //indicate the processor/driver is working correctly, by blinking the lights three times.
    for(i=0;i<=2;i++)
    {
        GPIO5 = 1;
        DelayMs(250);
        GPIO5 = 0;
    }
}
```

```

        DelayMs(250);
    }
}
void main()
{
    unsigned int uiCounter = 0; //time counter
    static bit bDark = 0; //true if dark enough, false otherwise
    static bit bLoBatt = 0; //true if battery is low, false otherwise
    init();
    while(1)
    {
        if (uiADC('B')>cBatHiThresh) //battery is registering good voltage
        {
            if (bLoBatt) //earlier battery was low
            {
                wait_seconds(cResponseDelayInSeconds);
                if (uiADC('B')>cBatHiThresh) //if the battery is still good
                {
                    bLoBatt = 0;
                }
            }
        }
        else
        {
            if (uiADC('B')<cBatLoThresh)
            {
                if (!bLoBatt) //earlier battery was good
                {
                    wait_seconds(cResponseDelayInSeconds);
                    if (uiADC('B')<cBatLoThresh) //if the battery is still bad
                    {
                        bLoBatt = 1;
                    }
                }
            }
        }
        if (uiADC('L')>cDarkHiThresh)
        {
            if (!bDark) //ambient lighting level dropped.
            {
                wait_seconds(cResponseDelayInSeconds); //delay the response to avoid
                jitter due to quick light level drops(e.g. due to a bird sitting on the detector)
                if (uiADC('L')>cDarkHiThresh) //if it is still dark...
                {
                    bDark = 1; //it's dark for sure
                }
            }
        }
        else
        {
            if (uiADC('L')<cDarkLoThresh) //fine tune these values
            {

```



## Appendix C – Field Illuminance Measurement Data

Dist. (m)	Lamp + Ambient (Lux)	Ambient (Lux)	Net Vertical Illum. (Lux)
-11	0.1	0	0.1
-10	0.29	0	0.29
-9	0.38	0	0.38
-8	0.42	0	0.42
-7	0.66	0.04	0.62
-6	1.1	0.03	1.07
-5	1.46	0.03	1.43
-4	5.2	0.06	5.14
-3	17	0.05	16.95
-2	20	0.07	19.93
-1	27	0.07	26.93
0	30	0.2	29.8
1	24	0.08	23.92
2	14.6	0.25	14.35
3	11.1	0.12	10.98
4	10.8	0.27	10.53
5	5	0.15	4.85
6	1.5	0.2	1.3
7	0.8	0.21	0.59
8	0.5	0.25	0.25
9	0.46	0.23	0.23
10	0.37	0.15	0.22
11	0.32	0.2	0.12
12	0.22	0.16	0.06

**Table C1 – Measured Vertical Illuminance Distribution along the Street**

Dist. (m)	Lamp + Ambient (Lux)	Ambient (Lux)	Net Vertical Illum. (Lux)
-3	0.2	0.1	0.1
-2	2	0.4	1.6
-1	10	1	9
0	32	1	31
1	32	1	31
2	20.5	1	19.5
3	2.5	1	1.5
4	0.59	0.1	0.49
5	0.5	0.1	0.4
6	0.2	0	0.2
7	0.45	0.27	0.18

**Table C2 – Measured Vertical Illuminance Distribution across the Street**

## References

- [1]. Douglas F. Barnes, Robert Van Der Plas and Willem Floor. “Tackling the Rural Energy Problem in Developing Countries”. *Finance and Development – International Monetary Fund*, pp. 11-15, June 1997
- [2]. John M. Anderson. “First Electric Street Lamps” *IEEE Power Engineering Review*, pp. 39-40, Mar. 2000.
- [3]. Unknown Author. “History of Street Lighting.” Internet:  
[http://en.wikipedia.org/wiki/Street\\_light](http://en.wikipedia.org/wiki/Street_light), Jan. 02, 2008 [Apr. 01, 2008].
- [4]. Illuminating Engineering Society of North America “IESNA RP-8-00” *American National Standard Practice for Roadway Lighting*, 2005
- [5]. Gordon S. Smith and Peter Barss. “Unintentional Injuries in Developing Countries: The Epidemiology of a Neglected Problem” *Epidemiologic Reviews - The Johns Hopkins University School of Hygiene and Public Health* Vol. 13, 1991
- [6]. John Klein. (2003, Apr) “Shoot-through in Synchronous Buck Converters.” *FairChild Semiconductor Application Note AN-6003* [Online]. Available:  
<http://www.fairchildsemi.com/an/AN/AN-6003.pdf> [Apr 01, 2008].
- [7]. Rob McMonagle. *The Environmental Attributes of Solar PV in the Canadian Context*. Internet: <http://www.cansia.ca/downloads/report2006/C21.pdf> [Apr 06, 2008] , The Canadian Solar Industries Association, Jul 2006
- [8]. Cree<sup>®</sup> XLamp<sup>®</sup> XR-E LED Data Sheet. Internet:  
<http://www.cree.com/products/pdf/XLamp7090XR-E.pdf>, Jan 2008 [Apr 06, 2008]

- [9]. PowerSonic Corporation. “PowerSonic Sealed Lead Acid Batteries – Technical Handbook”, Internet: [http://www.power-sonic.com/index.php?doc\\_id=116](http://www.power-sonic.com/index.php?doc_id=116), Jul, 1998 [Apr 09, 2008]
- [10]. Texas Instruments. “UC3843 Current Mode PWM Controller – Datasheet”, Internet: <http://focus.ti.com/docs/prod/folders/print/uc3843.html>, Jun 2007 [Apr 10, 2008]
- [11]. Aranzazu Diaz-Valdivieso, Dirk Ahlers, Gerald Deboy. “Relevance of P-Channel MOSFETs in Current and Future Applications”. *Power Electronics and Motion Control Conference, EPE-PEMC 2006. 12th International*, pp 1983-1987, Aug 2006.
- [12]. Julio Sanchez, Maria P. Canton. *Programming the Microchip PIC*. Boca Raton, FL: CRC Press, 2007
- [13]. Dogan Ibrahim. *Microcontroller Based Applied Digital Control*. West Sussex, England: John Wiley & Sons Ltd., 2006
- [14]. Richard Perez. “Lead-Acid Battery State of Charge vs. Voltage”. *Home Power*, vol 36, pp. 66-69, Aug/Sep 1993
- [15]. Joel Arnold. “When the Lights go Out: LED Failure Modes and Mechanisms”, Internet: [http://www.emsnow.com/cnt/files/White Papers/DFRLEDFailures.pdf](http://www.emsnow.com/cnt/files/White%20Papers/DFRLEDFailures.pdf) , Jun 2007 [Apr 16, 2008]
- [16]. Texas Instruments Inc. “Improved Charging Methods for Lead-Acid Batteries using the UC3906”, Internet: <http://www.ti.com/sc/docs/psheets/abstract/apps/slual15.htm>, Oct 1999 [Apr 16, 2008]
- [17]. Laszlo Balogh-Texas Instruments Inc. “Implementing Multi-State Charge Algorithm with the UC3909 Switch-mode Lead-Acid Battery Charger Controller”, Internet: <http://focus.ti.com/lit/an/slua098/slua098.pdf>, Aug 1997 [Apr 17 2008]

- [18]. L2Optics. “Flare Lens”, Internet: <http://www.l2optics.com/flare.aspx>, [Apr 17, 2008]
- [19]. Ziad Abu Amer. “An Overview of Social Conditions in the Refugee Camps”, *AMER Journal of Refugee Studies*. pp 149-151, Vol. 2 No.1, 1989
- [20]. Evan Mills. “The Role of High-Efficiency Lighting Systems in Meeting Humanitarian Needs in Camps for Refugees and Internally Displaced People”, Internet: [http://light.lbl.gov/pubs/pdf/Refugee\\_and\\_IDPs.pdf](http://light.lbl.gov/pubs/pdf/Refugee_and_IDPs.pdf), Aug 2003 [Apr 17, 2008]